Influences on the Accuracy of Torque Calculation for Permanent Magnet Synchronous Machines

Andreas Thul, Benedikt Groschup, and Kay Hameyer, *Senior Member, IEEE*

***Abstract*—In this work, the influences on the torque generated by permanent magnet synchronous machines are identified to provide approaches to improve the accuracy of torque calculation. By analyzing the torque generation mechanism, basic machine parameters influencing the generated torque are identified. The machine torque is split into different components, i.e. synchronous, reluctance, and parasitic torque components. The parasitic component results from non-linearities such as saturation. In a second step, environmental and operational conditions influencing those basic parameters are determined. Based on this analysis, the remanence flux density of the permanent magnets, the magnetization behavior of the soft-magnetic material, and the iron losses are selected for the study. Two traction drive machine designs are used in the parameter study. The machine torque is evaluated by performing 2D magnetostatic Finite-Element simulations of the investigated machine designs. The results show quantify the interdependencies between the torque components and the model parameters. The significance of the influence of the parameters on the accuracy of the torque calculation is discussed.**

***Index Terms*—PMSM torque calculation, accuracy of torque calculation, soft magnetic material, hard magnetic material, torque control.**

I. Introduction

THE torque of permanent magnet synchronous machines (PMSM) is basically controlled by feeding appropriate stator currents to the machine. For most drive trains operating with a speed controller, a fixed conversion between torque demand and stator currents can be used, since the outer speed control loop compensates model inaccuracies. Yet there are some applications, where the actual torque has to be controlled and an outer speed control loop is not usable. In hybrid drive trains with mechanical power split (e.g. [1] and [2]), the speed of the drive train is fixed by the vehicle speed. In this case, the power distribution has to be controlled by the torque of the electric drive. Another example is a single wheel drive, where each motor torque is controlled separately e.g. to stabilize vehicle dynamics. In most cases, the machine torque is not measured in these applications. Open loop torque control strategies based on models of the torque-currrent-dependency have to be used. Any error in the model will decrease the effectiveness of the underlying operation strategy. For the first example, the power distribution in hybrid drive trains would deviate from the desired ratio. For the second example, the stabilizing effect of the torque control on the vehicle dynamics could be compromised. An accurate calculation of the torque is indispensible for these applications.

Idealized machine models based on two-axis theory lead to a simple dependency between current and torque. The degree of idealization is high in this case, resulting in torque prediction errors. It is possible to extend the idealized models to consider many parasitic effects [3]. In such models, parameters such as inductances and flux linkages are dependent on current, rotor position and other properties. The torque prediction error of such models is determined by the uncertainties of the underlying magnetic field calculation. There are few studies, which examine the influence on torque for certain single parameters and effects. As stated in [4], saturation has a considerable influence on the torque. In [5], a relative torque error of up to 30% is stated for a certain machine design. For a different design, the maximum torque error due to saturation is identified to 5% by [6]. The significance of the influence of saturation on Maximum-torque-per-Ampere (MTPA) control stategies is shown e.g. in [7]–[9]. Yet, the studies do not include the influence of different machine designs. Further, it is not discussed which material properties are responsible for the influence of saturation on torque. Therefore, it is difficult to evaluate the accuracy of the control strategies shown in [7]–[9].

The accurate calculation of iron loss [10], which can also be expressed as a loss torque, is a frequently discussed topic for electric machine modeling. The influence of iron loss on the torque is examined by [11] and [12]. In [11], the torque deviation due to iron losses is quantified as 5–30%. In [12], the error was given as 5% in the base speed region and rises up to 20% in the field weakening region.

The trend of designing high speed electric traction drives leads to high electric fundamental frequencies in the machine [2]. The influence of the soft magnetic material selection on the iron loss and thus the loss torque influence in dependency of the electric frequency is already discussed in literature [13]. An in-depth analysis of the influence of the frequency on the magnetization curve of the material is not performed. An investigation of the influence of different machine designs in combination with the

Manuscript received December 29, 2019; revised May 28, 2020; accepted July 9, 2020. Date of publication July 15, 2020; date of current version November 24, 2020. Paper no. TEC-01276-2019. *(Corresponding author: Andreas Thul.)*

The authors are with the Institute of Electrical Machines, RWTH Aachen University, 52056 Aachen, Germany (e-mail: andreas.thul@iem.rwth-aachen.de; benedikt.groschup@iem.rwth-aachen.de; kay.hameyer@iem.rwth-aachen.de).

Color versions of one or more of the figures in this article are available online at https://ieeexplore.ieee.org.

Digital Object Identifier 10.1109/TEC.2020.3009490

frequency influence on the magnetization curve cannot be found in literature.

Another frequently discussed influence on the torque of electric machines is the polarization of the permanent magnets. The temperature of the magnets influences the polarization of the material as shown in [14]. The stand of the art literature does not include the influence of this quantity under consideration of different machine designs and for different operational conditions of the machine.

The influence of manufacturing tolerances is examined e.g. in [15] or [16]. Yet the main focus in both studies lies on parasitic effects such as cogging torque. The average torque is not examined explicitly.

From the differences between the amount of torque errors reported in the mentioned studies, it can be derived, that the quantitative influence of every effect on the torque has to be dependent on machine parameters and properties. Thus for every design, the importance of certain effects on the torque prediction accuracy can vary. Therefore, it is difficult to obtain reliable a-priory torque calculations during the design process, since it is unclear which phenomena have to be included in the calculation to ensure a sufficient accuracy. A comprehensive analysis of different influencing factors on the torque and their interaction is missing.

The aim of this study is to overcome the stated problems by performing a well-structured analysis, how the machine torque is influenced. In a first step, the basic machine parameters having a direct influence on the electromagnetic torque are identified. These basic influencing properties themselves depend on other machine parameters, parasitic effects, design aspects, material properties or environmental conditions. The second step of the analysis is the identification of those secondary influencing parameters and the quantification of their sensitivity. Quantitative influences will be calculated for a significant selection of parameters. To include influences of the PMSM topology, this step will be performed for two different designs. By comparing the resulting torque deviations, it can be determined, which influencing paths are more or less important for certain designs or operational conditions.

The rest of this paper is organized as follows: In section two, possible influencing parameters are derived in two steps as described above. In the third section, a selection of parameters which shall be investigated further is done. For each parameter, a suitable range of variation is derived. The analysis results are presented and discussed in section four. Finally, a conclusion is given.

II. Torque Components and Possible Influencing Properties

A. Primary Influences on the Electromagnetic Torque

The electromagnetic torque of PMSM machines is in general produced by the interaction of stator and rotor flux linked through the air gap. Considering non-idealities such as saturation and cross-coupling, the following torque equation can be derived [3]:

$$T = T_{\mathrm{sync}} + T_{\mathrm{rel}} + T_{\mathrm{cc},1} + T_{\mathrm{cc},2} \tag{1}$$

$$T_{\mathrm{sync}} = \frac{3 \cdot p}{2} \cdot \psi_{\mathrm{F,d}}(i_{\mathrm{d}}, i_{\mathrm{q}}) \cdot i_{\mathrm{q}} \tag{2}$$

$$T_{\mathrm{rel}} = \frac{3 \cdot p}{2} \cdot \left[L_{\mathrm{dd}}(i_{\mathrm{d}}, i_{\mathrm{q}}) - L_{\mathrm{qq}}(i_{\mathrm{d}}, i_{\mathrm{q}})\right] \cdot i_{\mathrm{d}} \cdot i_{\mathrm{q}} \tag{3}$$

$$T_{\mathrm{cc},1} = -\frac{3 \cdot p}{2} \cdot \psi_{\mathrm{F,q}}(i_{\mathrm{d}}, i_{\mathrm{q}}) \cdot i_{\mathrm{d}} \tag{4}$$

$$T_{\mathrm{cc},2} = \frac{3 \cdot p}{2} \cdot L_{\mathrm{d,q}}(i_{\mathrm{d}}, i_{\mathrm{q}}) \cdot (i_{\mathrm{d}}^2 - i_{\mathrm{q}}^2). \tag{5}$$

The total torque of the machine T is the sum of the synchronous torque T_{sync}, the reluctance torque T_{rel}, and the parasitic cross-coupling torque contents $T_{\mathrm{cc},1}$ and $T_{\mathrm{cc},2}$. For the calculation of the torque contents, the number of pole pairs p, the current in the d-axis i_{d} and in the q-axis i_{q} are used. $L_{\mathrm{dd}}(i_{\mathrm{d}}, i_{\mathrm{q}})$ and $L_{\mathrm{qq}}(i_{\mathrm{d}}, i_{\mathrm{q}})$ represent the current-dependent self inductances in the d-q reference frame. $L_{\mathrm{dq}}(i_{\mathrm{d}}, i_{\mathrm{q}})$ is the mutual inductance between d- and q-axis, representing parasitic cross-coupling within the stator. $\psi_{\mathrm{F,d}}(i_{\mathrm{d}}, i_{\mathrm{q}})$ represents the part of the permanent magnet rotor flux linked to the stator d-axis. Due to cross-coupling, a small portion of the rotor flux is also linked to the q-axis. This flux linkage is described by $\psi_{\mathrm{F,q}}(i_{\mathrm{d}}, i_{\mathrm{q}})$. Inductances and flux linkages in (1)–(5) are referenced in the following as the primary influences on the machine torque. Within this model framework, any torque uncertainty can be linked to changing values of this parameters. Yet, depending on the calculation method, further influences can appear due to unmodeled phenomena. One example are the iron losses. The iron losses are calculated using post-processing routines like the IEM loss formula [17]. Since the field solution is not affected by post processing routines, effects of iron losses on torque have to be modeled by an additional torque component. Saturation, or the nonlinear magnetic material behavior in general, can be studied as a primary influencing factor due to its influence on all quantities in (1)-(5). The cross coupling inductance L_{dq} itself is a consequence of saturation in the magnetic cirquit [18], [19]. As described in [20], the q-axis excitation flux linkage $\psi_{\mathrm{F,q}}$ can be explained by saturation as well.

B. Secondary Influencing Parameters

Since $\psi_{\mathrm{F,d}}$ and $\psi_{\mathrm{F,q}}$ are generated by permanent magnets, it is clear that the magnet material properties have a significant influence on torque, namely the synchronous part. The main property responsible for the amount of permanent magnet flux is the remanence induction, which has a strong temperature dependency. The rotor temperature can change during operation due to the losses produced inside the machine. Since measuring the temperature of the rotor is a complex task, temperature changes cause considerable uncertainties of the produced torque. The influence will be calculated in detail in the following sections. Besides the temperature influence, changes in material properties due to production are important sources for uncertainties

regarding the remanence induction. The magnetizing process can lead to variations in the resulting excitation flux linkage [21].

Commonly, a constant relative permeability is assumed for modeling the magnet material. In order to avoid irreversible demagnetization, the operating range of the machine is limited and the magnetic circuit is designed to avoid magnet degaussing below the linear region. This assumption is valid for the machine designs examined here. The coercitive field strength is considered less important and is not examined in this work. For other machine designs which are operating close to irreversible demagnetization, this assumption might be invalid. In general, the magnetic behavior of stator and rotor lamination influence the amount of rotor flux linked to the stator. Although the magnetic resistance of the flux path through stator and rotor is dominated by the air gap, stray paths do not leave the rotor iron in interior permanent magnet machines. Therefore, some influence of the rotor iron magnetizing behavior on the synchronous torque can be expected.

The inductances L_{dd}, L_{dq} and L_{qq} are mainly dependent on the behavior of the soft magnetic rotor and stator material and the different magnetic resistances in d- and q-axis. Due to the nonlinear material behavior, the inductances can also be influenced by the rotor flux. Concerning the magnetic circuit, significant changes in the geometric dimensions are not expected to occur. Yet the question arises whether different rotor magnet designs behave differently regarding the other influencing factors.

III. Description of Studied Influences

Based on the analysis in the previous section, the following set of secondary influencing parameters is selected for a quantitative analysis:

- Changes of stator and rotor iron saturation polarization
- Magnetization frequency of the soft magnetic material
- Remanence induction of permanent magnets
- Influence of rotor design

A. Saturation of the Polarization of the Soft Magnetic Material

The saturation of the polarization J_{s} of the soft magnetic material in the electric machine simulation can be influenced by both physical influences of the material as well as numerical and experimental inaccuracies in the material measurement and its pre-processing procedure. An example for a physical influence are the alloy constituents. The dependency of J_{s} on the silicon content x_{Si} and aluminum content x_{Al} is given in [22]

$$J_{\mathrm{s}} = 2.162T - 0.043x_{\mathrm{Si}} - 0.0625x_{\mathrm{Al}}. \tag{6}$$

An example for inaccuracies in the measurement and preprocessing procedure of the machine simulation are inaccuracies resulting from the Kennelly approximation. The measured magnetic flux density B for different field strengths H can be extrapolated using following formulation [23]:

$$B = \frac{H}{a + b \cdot H}, \tag{7}$$

with a and b being coefficients that needs to be identified in the extrapolation process.

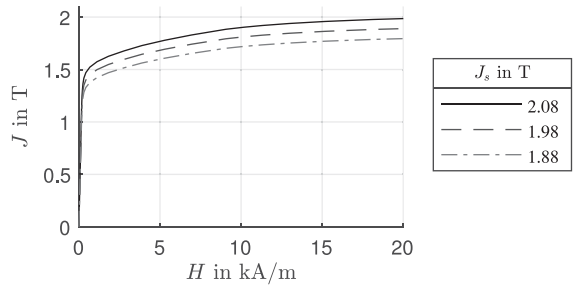

Fig. 1. Studied magnetization curves for different saturations J_{s}.

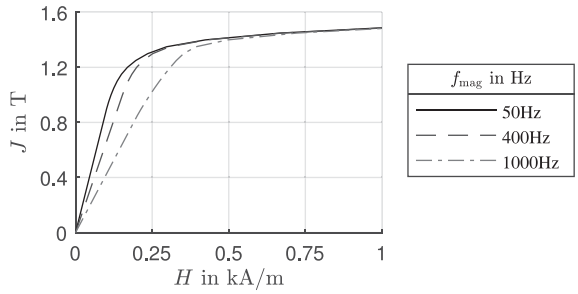

Fig. 2. Studied magnetization curves for different frequencies f_{mag}.

In this study, the influence of different saturation of the polarization of the soft magnetic material should be studied. Therefore, the magnetic properties of a M270-35 A sheet are measured using a single sheet tester [24]. A polarization frequency of 400 Hz and a polarization J from 0.1 T up to 1.7 T is used in the measurements. Measurements parallel and perpendicular to the rolling direction are performed and the mean value is calculated. The saturation of the polarization is calculated using (6), resulting in $J_{\mathrm{s}} = 1.98T$. For the extrapolation of the measured polarization up to the saturation value J_{s}, (7) is used. The resulting magnetization curve $J(H)$ is used as a reference in the study. Two magnetization curves $J'(H)$ for comparison are generated based on the simplified assumption:

$$J'(H) = J(H) \cdot \frac{J'_{\mathrm{s}}}{J_{\mathrm{s}}}, \tag{8}$$

with J'_{s} is equal to $1.88T$ and $2.08T$. The three different magnetization curves in dependency of the saturation of polarization J_{s} are depicted in Fig. 1. The studied magnetization curves do not represent real material behavior, but can be used to investigate the saturation influence in the machine simulation process.

B. Magnetization Frequency of the Soft Magnetic Material

A second characteristic parameter of the magnetization curve that influences the machine performance is the reluctivity for low magnetic field strengths. This value is influenced for example by the magnetization frequency f_{mag} of the soft magnetic material. In order to investigate the influence, previously described measurement procedure with $f_{\mathrm{mag}} = 400$ Hz is repeated for 50 Hz and 1000 Hz. The magnetization curves used in the study are depicted in Fig. 2.

TABLE I
MATERIAL PARAMETERS OF MEASURED VACODYM 890 AP IN [14]

Variable	Value	Variable	Value
α_1 in 1/K	-1.12e-3	$B_\mathrm{r}(T_0 = 20\,^\circ\mathrm{C})$ in T	1.118
α_2 in 1/K^2	-1.72e-6	$B_\mathrm{r}(T = 100\,^\circ\mathrm{C})$ in T	1.006
T_0 in °C	20	$B_\mathrm{r}(T = 180\,^\circ\mathrm{C})$ in T	0.868

TABLE II
OVERVIEW OF THE STUDIED MACHINE DESIGNS

Variable	Design 1	Design 2
Number of pole pairs p	6	4
Peak torque $T_\mathrm{max}$in Nm	250	450
Max. rotational speed n_max in rpm	11400	16500
Max. el. fund. frequency f_el in Hz	1140	1100

The resulting polarization J is influenced for low magnetic field strength H up to 500 Am^{-1}. After this value is reached, the three studied magnetization curves converge. Note that this effect occurs for significantly lower values of H, which can be seen from the different maximum values of the x-axis in Fig. 2 in comparison to Fig. 1.

C. Magnetic Flux of the Permanent Magnets

Another parameter that influences the machine characteristics is the magnetic flux of the permanent magnets. This flux influences the rotor flux linked to the stator. Possible influences on this parameter are the material properties and the operational temperature of the magnets. The latter case is used as an example to evaluate upper and lower limits for the study. The dependency of the magnet temperature T_pm on the remanence flux density of the magnets B_r can be described by a non linear analytical formulation as shown in [14]

$$B_\mathrm{r} = B_\mathrm{r}(T_0) \cdot (1 + \alpha_1(T_\mathrm{pm} - T_0) + \alpha_2(T_\mathrm{pm} - T_0)^2), \quad (9)$$

with the fitting parameters α_1 and α_2. In this study, the material Vacodym 890 AP with the measurement procedure and measurement results as described in [14] is used. The values of the parameters as well as the resulting remanence flux density is shown in Table I. In a temperature range of 20 °C up to 180 °C, the value of the remanence flux density of the material B_r decreases from $1.118T$ to $0.868T$.

D. Studied Electric Machine Designs

In order to evaluate the influences of the parameters for different permanent magnet synchronous machine designs, two different designs are selected. Both machines have internal rotors, burried magnets and are designed for the purpose of an electric machine traction drive. An overview of the technical data of both machines is given in Table II.

A comparison of the axial view of the two different machine designs is given in Fig. 3. Design 1 is equipped with a double layered buried magnet. Design 2 is equipped with a V-shaped rotor. Additional punches are inserted into the rotor lamination of design 1 in order to realize a high difference in the self inductance in the d-q reference frame $L_\mathrm{dd}(i_\mathrm{d}, i_\mathrm{q})$ and $L_\mathrm{qq}(i_\mathrm{d}, i_\mathrm{q})$. This measure helps to realize adequate reluctance torque content T_rel.

Fig. 3. Axial view of the lamination of Design 1 (left) and Design 2 (right).

TABLE III
SIMULATION PLAN

Simulation	Design	J_s' in T	f_mag in Hz	T_pm in °C
V111 (ref.)	Design 1	1.98	400	100
V211	Design 1	1.88	400	100
V221	Design 1	2.08	400	100
V311	Design 1	1.98	50	100
V321	Design 1	1.98	1000	100
V411	Design 1	1.98	400	20
V421	Design 1	1.98	400	180
V112 (ref.)	Design 2	1.98	400	100
V212	Design 2	1.88	400	100
V222	Design 2	2.08	400	100
V312	Design 2	1.98	50	100
V322	Design 2	1.98	1000	100
V412	Design 2	1.98	400	20
V422	Design 2	1.98	400	180

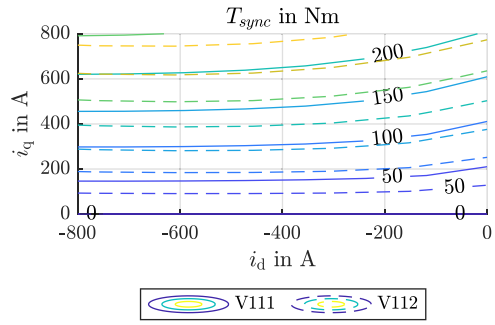

Fig. 4. Comparison of synchronous torque T_sync for both machine designs.

IV. SIMULATION RESULTS AND DISCUSSION

For the study, reference parameter values for J_s', f_mag and T_pm are set. Each parameter is varied independently to examine the influence individually. This results in a total of seven cases for each machine design as shown in Table III. A three-digit ID is assigned to each case. The first digit indicates which parameter is changed from its reference value (1: none, 2: J_s', 3: f_mag, 4: T_pm). The second digit indexes the changed parameter values and the third digit indicates the machine design. FE simulations are carried out using the inhouse iMOOSE/pyMOOSE solver package. For each case, the currents i_d and i_q are varied.

A. Torque Components and Saturation Influence

In Figs. 4–7, the different torque components are displayed in the in the stator current plane $(i_\mathrm{d}, i_\mathrm{q})$ for both machine designs. The synchronus torque T_sync increases when field-weakening currents are applied. Due to the reduced flux density level

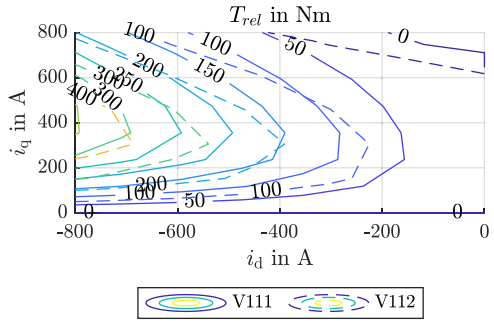

Fig. 5. Comparison of reluctance torque T_{rel} for both machine designs.

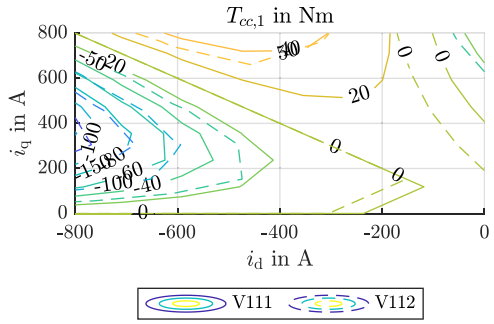

Fig. 6. Comparison of parasitic torque $T_{\mathrm{cc},1}$ for both machine designs.

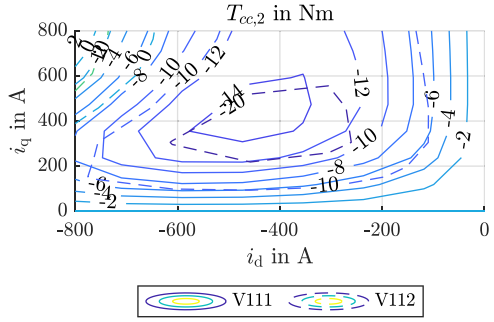

Fig. 7. Comparison of parasitic torque $T_{\mathrm{cc},2}$ for both machine designs.

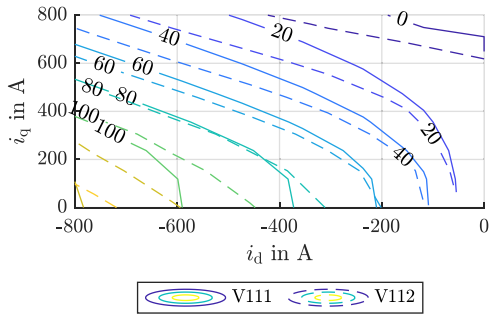

Fig. 8. Ratio of relutance to overall torque for both machine designs.

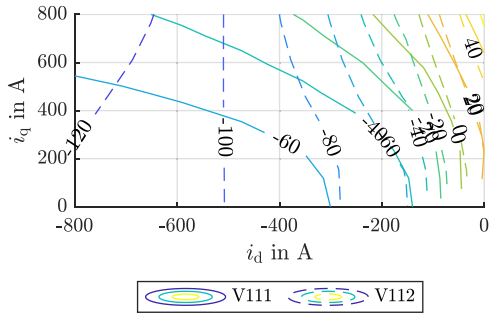

Fig. 9. Overall torque deviation caused by saturation.

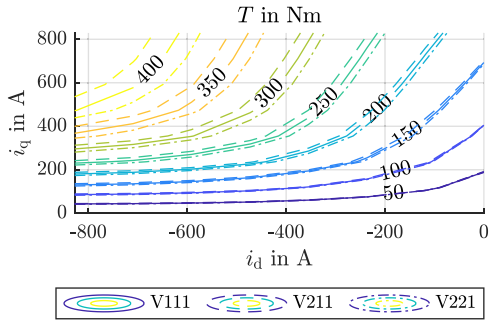

Fig. 10. Torque isolines for different saturation Polarization values.

inside the material, the nonlinearity is reduced and T_{sync} is mainly depending on i_{q}. For the same reason the reluctance torque also increases in field-weakening operation. The parasitic excitation flux in the q axis causes $T_{\mathrm{cc},2}$, which slightly reduces the generated torque. The influence of L_{dq} on the overall torque is more significant. Especially for high field-weakening currents, the overall torque will be significantly overestimated, if $T_{\mathrm{cc},1}$ is not considered. The relative amount of the reluctance torque is shown in Fig. 8. Values larger than 1 are caused by negative values of the parasitic torque components.

A comparison of both machines shows, that the basic coherences are the same for both machines. In order to evaluate the overall influence of saturation effects, the torque is recalculated by using average values for inductances and flux linkages and neglecting both parasitic torque components. The resulting relative torque deviation compared to the overall torque considering saturation is shown in Fig. 9. It is clear, that omitting saturation leads to large deviation, especially in the field-weakening region. Here, it can be observed that the overall saturation influence on torque is larger for machine design two.

B. Influence of Material Properties

In Figs. 10–12, the torque isolines in the stator current plane $(i_{\mathrm{d}}, i_{\mathrm{q}})$ are depicted for the different cases. In Fig. 13, the maximum values of the relative torque differences

$$\max\left(\frac{T_{\mathrm{a,xyz}} - T_{\mathrm{sum,111}}}{T_{\mathrm{sum,111}}}\right), \tag{10}$$

where "a" denotes either the overall torque or one of the four torque components defined in (2–5), are given. Increasing the saturation polarization will shift the torque isolines to lower current values, whereas a lower saturation polarization will lead

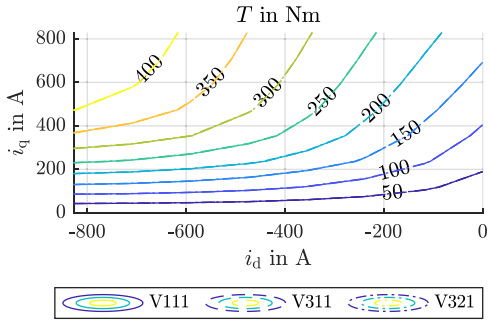

Fig. 11. Torque isolines for different saturation frequencies.

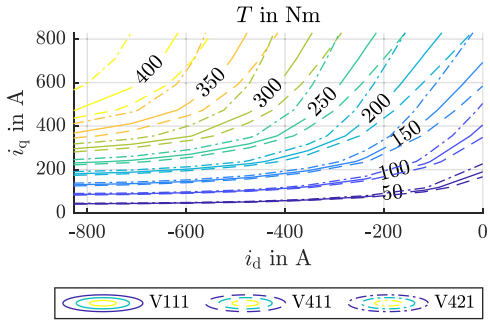

Fig. 12. Torque isolines for different saturation rotor temperature values.

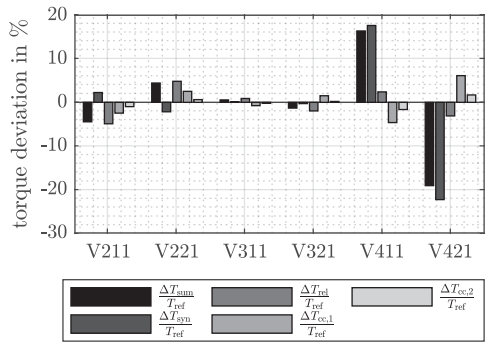

Fig. 13. Maximum relative torque deviations compared to the correponding reference torque values.

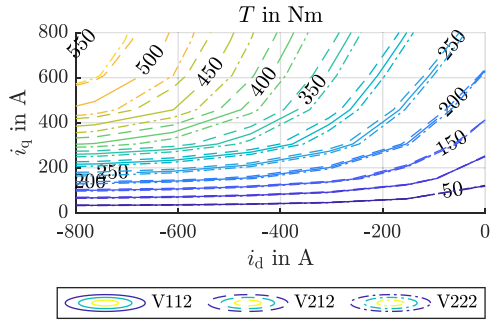

Fig. 14. Torque isolines for different saturation Polarization values.

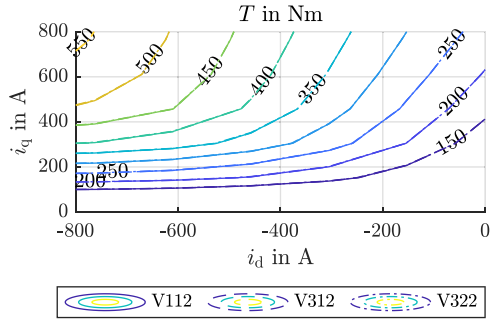

Fig. 15. Torque isolines for different saturation frequency values.

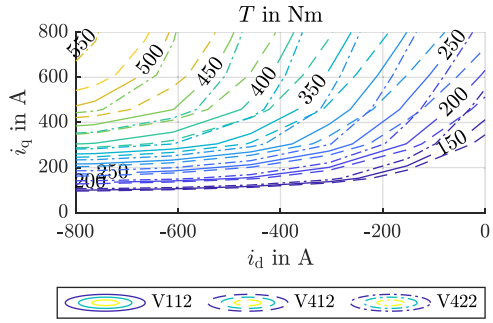

Fig. 16. Torque isolines for different saturation rotor temperature values.

to smaller torque values at a given current operating point. The comparison of torque components shows that a reduced J_s also reduced the reluctance torque, whereas the synchronous torque is increased. The latter can be explained by an decrease in stray flux, since the magnet holding bridges are saturated earlier. In summary, the effect on reluctance torque is dominant, the overall torque changes up to 4.5%. Changing the magnetizing frequency and thus shearing the magnetization curve has no significant direct effect on the electromagnetic torque. Considering the fact that iron losses lead to a torque reduction, a sheared magnetization curve can indirectly influence the machine torque due to increased iron losses.

The a change in the rotor magnet temperature within the specified operation limits lead to torque changes up to 19.1% compared to the reference case. Altogether, permanent magnet remanence induction is the most important material property regarding torque, affecting especially all rotor flux-related torque components.

The same evaluation is performed for the second machine (Figs. 14–17). As before, the influence of the magnetizing frequency on the torque is quite small. Compared to the first machine design, the torque deviations caused by magnet temperature and saturation polarization changes are slightly increased.

C. *Influence of Iron Losses on Torque*

As described above, the influence of iron losses on the torque has to be modeled by an additional torque component. This torque component is calculated in the post processing and is denoted as loss torque. Since the iron losses depend on the frequency, the loss torque cannot be examined solely in the current space vector plane. Instead, the actual operating points within

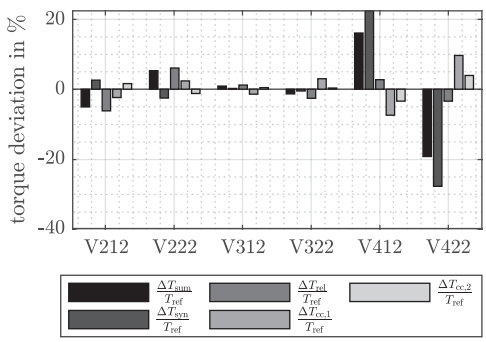

Fig. 17. Maximum relative torque deviations compared to the correponding reference torque values.

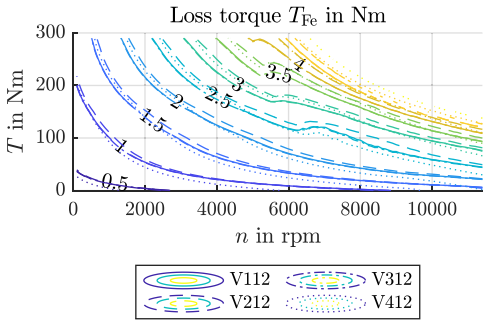

Fig. 18. Torque reduction due to iron losses of Machine design 2 in the speed-torque plane.

the torque-speed plane have to be calculated. The respective current components $(i_{\mathrm{d}}, i_{\mathrm{d}})$ for each operating point are chosen by applying the MTPA (Maximum torque per ampere) principle to minimize the stator current under consideration of the stator voltage limit as described in [25]. The resulting loss torque for machine design 2 and one variation of each studied influencing parameter is shown in Fig. 18. The occurring loss torque values are small compared to the maximum machine torque. Therefore, it can be concluded that iron losses are no significant influencing factor for this machine. It is important to keep in mind, that this cannot be generalized. Especially for smaller machines, which operate at higher speeds and produce less torque, iron losses are expected to have more influence. Despite the small influence on overall torque for this machine design, some basic conclusions regarding the influence of the varied parameters on the loss torque itself can be drawn. Reducing the saturation polarization of the soft magnetic material (V212) will shift the loss torque contour lines to higher powers and therefore reduce the loss torque for any given operating point. Any shearing of the magnetization curve (V312) has little influence on the loss toque. It is important to keep in mind the post-processing nature of loss calculation. The used loss model is frequency dependent and therefore always takes into account the frequency dependency of the iron looses. The effect of a reduced rotor temperature (and therefore increased remanence induction) depends on the operating point. In field weakening region, loss torque is increased. Yet in the base speed region, loss torque will decrease if the machine is operated at high toque values.

V. Conclusion

Based on a torque equation for permanent magnet synchronous machines including the nonlinear magnetic circuit behavior, possible influence paths causing uncertainties regarding torque have been identified. Due to saturation effects, additional torque components have to be considered beside reluctance and synchronous torque. A set of influencing paths has been chosen for a detailed quantitative analysis. Two machine designs, one with V-shaped magnets and one with PMSynRM type rotor, were chosen for comparison. For the permanent magnet material, the remanence induction was varied based on its temperature dependency by applying the operational temperature limits specified for the machines. A variation of the saturation of the soft magnetic material polarization and magnetizing frequency was performed. For these cases, a parameter variation was performed. The remanence induction was identified as the parameter with the most significant influence on the torque. It directly changes the synchronous torque, as expected. Other torque components are affected as well due to the cross coupling with the local field distribution in the machine. Regarding the soft magnetic behavior of the rotor and stator iron, results indicated that the saturation polarization has a significant effect on the reluctance torque. In contrast, the reduced permeability in the low-magnetized region caused by an increased magnetizing frequency has only little effect on the torque. The comparison of results for both machines did not indicate any major differences regarding quantitative and qualitative influences on torque. It is therefore expected, that the stated basic coherences are applicable to other PMSM machine designs with salient rotor designs, at least if the magnetic utilization is similar. In comparison to [5] and [6], the overall influence of saturation effects on the torque is higher for the machine designs studied here. Regarding iron losses, the overall influence an torque for the given machines is small. Other investigations have reported higher influences. As explained above, this is expected for smaller machine designs operating at higher speeds as studied in [11].

References

[1] M. Nell, D. Butterweck, O. Eryilmaz, and K. Hameyer, "Design of a 48 V electric all-wheel-drive system for a hybrid vehicle," in *Proc. IEEE Transp. Electrific. Conf. Expo.*, 2018, pp. 513–518.

[2] D. Butterweck, M. Hombitzer, and K. Hameyer, "Multiphysical design methodology of a high-speed induction motor for a kinematic-electric powertrain," in *Proc. IEEE Int. Electric Mach. Drives Conf.*, 2017, pp. 1–6.

[3] T. Herold, D. Franck, E. Lange, and K. Hameyer, "Extension of a D-Q model of a permanent magnet excited synchronous machine by including saturation, cross-coupling and slotting effects," in *Proc. IEEE Int. Electric Mach. Drives Conf.*, 2011, pp. 1363–1367.

[4] M. Barcaro, N. Bianchi, and F. Magnussen, "Remarks on torque estimation accuracy in fractional-slot permanent-magnet motors," *IEEE Trans. Ind. Electron.*, vol. 59, no. 6, pp. 2565–2572, Jun. 2012.

[5] M. M. Bech, T. S. Frederiksen, and P. Sandholdt, "Accurate torque control of saturated interior permanent magnet synchronous motors in the field-weakening region," in *Proc. Conf. Rec. IEEE Ind. Appl. Conf.*, 2005, pp. 2526–2532.

[6] A. Soualmi, F. Dubas, D. Depernet, A. Randria, and C. Espanet, "Inductances estimation in the D-Q axis for an interior permanent-magnet synchronous machines with distributed windings," in *Proc. IEEE Int. Conf. Elect. Mach.*, 2012, pp. 308–314.

[7] Z. Li and H. Li, "MTPA control of PMSM system considering saturation and cross-coupling," in *Proc. 15th Int. Conf. Elect. Mach. Syst.*, 2012, pp. 1–5.

[8] H. Ge, B. Bilgin, and A. Emadi, "Global loss minimization control of PMSM considering cross-coupling and saturation," in *Proc. IEEE Energy Convers. Congr. Expo.*, 2015, pp. 6139–6144.
[9] A. Rabiei, T. Thiringer, M. Alatalo, and E. A. Grunditz, "Improved maximum-torque-per-ampere algorithm accounting for core saturation, cross-coupling effect, and temperature for a PMSM intended for vehicular applications," *IEEE Trans. Transp. Electrific.*, vol. 2, no. 2, pp. 150–159, Jun. 2016.
[10] G. von Pfingsten, A. Ruf, S. Steentjes, M. Hombitzer, D. Franck, and K. Hameyer, "Operating point resolved loss computation in electrical machines," *Archives Elect. Eng.*, vol. 65, no. 1, pp. 73–86, Mar. 2016.
[11] N. Urasaki, T. Senjyu, and K. Uezato, "Investigation of influences of various losses on electromagnetic torque for surface-mounted permanent magnet synchronous motors," *IEEE Trans. Power Electron.*, vol. 18, no. 1, pp. 131–139, Jan. 2003.
[12] T. Senjyu, N. Urasaki, and K. Uezato, "Influence of stator iron loss in flux weakening region for interior PMSM," in *Proc. IEEE Int. Conf. Power Electron. Drives Energy Syst. Ind. Growth*, 1998, pp. 20–25.
[13] A. Ruf, S. Steentjes, G. von Pfingsten, T. Grosse, and K. Hameyer, "Requirements on soft magnetic materials for electric traction motors," in *Proc. Conf. 7th Int. Conf. Magnetism Metall.*, 2016, pp. 111–128.
[14] N. Leuning, S. Elfgen, B. Groschup, G. Bavendiek, S. Steentjes, and K. Hameyer, "Advanced soft- and hard-magnetic material models for the numerical simulation of electrical machines," *IEEE Trans. Magn.*, vol. 54, no. 11, pp. 1–8, Nov. 2018.
[15] M. A. Khan, I. Husain, R. Islam, and J. Klass, "Design of experiments to address manufacturing tolerances and process variation influencing cogging torque and back emf in the mass production of the permanent magnet synchronous motors," in *Proc. IEEE Energy Convers. Congr. Expo.*, 2012, pp. 3032–3039.
[16] C. Mülder, M. Franck, M. Schröder, M. Balluff, A. Wanke, and K. Hameyer, "Impact study of isolated and correlated manufacturing tolerances of a permanent magnet synchronous machine for traction drives," in *Proc. IEEE Int. Electric Mach. Drives Conf.*, 2019, pp. 982–987.
[17] D. Eggers, S. Steentjes, and K. Hameyer, "Advanced iron-loss estimation for nonlinear material behavior," *IEEE Trans. Magn.*, vol. 48, no. 11, pp. 3021–3024, Nov. 2012.
[18] P. Vas, K. E. Hallenius, and J. E. Brown, "Cross-saturation in smooth-air-gap electrical machines," *IEEE Trans. Energy Convers.*, vol. EC-1, no. 1, pp. 103–112, Mar. 1986.
[19] A. M. El-Serafi and J. Wu, "Determination of the parameters representing the cross-magnetizing effect in saturated synchronous machines," *IEEE Trans. Energy Convers.*, vol. 8, no. 3, pp. 333–342, Sep. 1993.
[20] Y. Shi, J. Chai, X. Sun, and S. Mu, "Detailed description and analysis of the cross-coupling magnetic saturation on permanent magnet synchronous motor," *J. Eng.*, vol. 2018, no. 17, pp. 1855–1859, 2018.
[21] P. Offermann, I. Coenen, and K. Hameyer, "Consideration of erroneous magnets in the electromagnetic field simulation," in *Proc. 15th Int. IGTE Symp. Numer. Field Calculation Elect. Eng.*, 2012, p. 64.
[22] T. Yonamine and F. J. Landgraf, "Correlation between magnetic properties and crystallographic texture of silicon steel," *J. Magn. Magn. Mater.*, vol. 272–276, pp. E565 – E566, 2004.
[23] D. Jiles, *Introduction to Magnetism and Magnetic Materials*. 3rd ed. Boca Raton, FL, USA: CRC Press, 2015.
[24] DIN German Institute for Standardization, "Magnetic materials - part 3: Methods of measurement of the magnetic properties of electrical steel strip and sheet by means of a single sheet tester (IEC 60404-3:2010-5)," 2010.
[25] A. Ruf, S. Steentjes, A. Thul, and K. Hameyer, "Stator current vector determination under consideration of local iron loss distribution for partial load operation of PMSM," *IEEE Trans. Ind. Appl.*, vol. 52, no. 4, pp. 3005–3012, Jul./Aug. 2016.

Andreas Thul received the diploma degree in electrical engineering from RWTH Aachen University, Aachen, Germany, in 2013. He has been working as a Research Associate with the Institute of Electrical Machines, RWTH Aachen University, since October 2013. His current research interests include control of electrical machines, electric linearmotors, and measurement techniques for the characterization of soft magnetic materials.

Benedikt Groschup recieved the master's degree in automotive engineering and transport, in September 2015 at RWTH Aachen University. He started working as a Research Associate of RWTH Aachen University in February 2016. His current research interests include induction and permanent magnet motor modeling, iron loss calculation in macroscopic scale, vehicle modeling and thermal modeling.

Kay Hameyer (Senior Member, IEEE) received the M.Sc. degree in electrical engineering from the University of Hannover and the Ph.D. degree from the Berlin University of Technology, Germany. After his university studies, he worked with the Robert Bosch GmbH in Stuttgart, Germany as a Design Engineer for permanent magnet servo motors and vehicle board net components. From 1996 to 2004 Dr. Hameyer was a Full Professor for Numerical Field Computations and Electrical Machines with the KU Leuven in Belgium. Since 2004, he is Full Professor and the Director of the Institute of Electrical Machines (IEM) at RWTH Aachen University in Germany. 2006 he was Vice Dean of the faculty and from 2007 to 2009 he was the Dean of the faculty of Electrical Engineering and Information Technology of RWTH Aachen University. His research interests are numerical field computation and optimization, the design and controls of electrical machines, in particular permanent magnet excited machines and induction machines. Since several years Dr. Hameyer's work is concerned with magnetically excited audible noise in electrical machines, the life time estimation of insulating systems and the characterization of ferro-magnetic materials. Dr. Hameyer is author of more than 250 journal publications, more than 700 international conference publications and author of four books. Dr. Hameyer is a Member of VDE, IEEE Senior Member Fellow of the IET.